Modelling changes in soil structure caused by livestock treading

Alejandro Romero-Ruiz[1], Ross Monaghan[2], Alice Milne[1], Kevin Coleman[1], Laura Cardenas[3], Carmen Segura[4], and Andrew Whitmore[1]

1 Net zero and resilient farming, Rothamsted Research, Harpenden, United Kingdom
2 Invermay Agricultural Research Centre, AgResearch, Mosgiel, New Zealand
3 Net zero and resilient farming, Rothamsted Research, North Wyke, United Kingdom
4 Sustainable soils and crops, Rothamsted Research, North Wyke, United Kingdom

HIGHLIGHTS

- Soil compaction increases bulk density and reduces saturated hydraulic conductivity
- A soil rheology and animal movement models estimate changes in these properties
- The model predicts changes in macroporosity and saturated hydraulic conductivity
- Compaction-induced changes in these soil properties depend on the soil water content
- Predicted temporal changes in soil properties are validated with literature data

KEYWORDS

soil compaction - animal treading - soil structure - hydraulic conductivity - bulk density - macroporosity

Abstract

Increased soil compaction resulting from livestock treading and use of heavy machinery is a major environmental hazard often linked to degradation of the soil ecosystem and economic services. However, there is a weak quantitative understanding of the spatial and temporal extent of soil compaction and how it modifies soil properties and associated functions. To address this challenge, we developed a framework for systematic modelling soil compaction caused by grazing animals. We considered random movement of livestock in a confined field to describe the spatial variation in the soil that is discretized in square cells with given properties. We then used a rheology model based on Bingham's law to infer compaction-induced changes in soil bulk density and porosity. An associated reduction of saturated hydraulic conductivity is obtained from soil porosity predictions by empirically accounting for macroporosity reduction using a dual-porosity permeability model. This model is coupled with an empirical model of soil structure recovery to account for biological activity (i.e., earthworms and roots). The modelling framework effectively captures primary effects of soil compaction on key soil properties despite lack of explicit consideration of complex effects of compaction such as redistribution of pore sizes and changes in pore connectivity. We tested the model using bulk density, macroporosity and saturated hydraulic conductivity data from a grazing study at the Tussock Creek experimental platform in New Zealand. Data were successfully reproduced by the model. Compaction and recovery trends can be interpreted in terms of model properties associated with management, soil texture and environmental conditions. If data are available for calibration of such properties, the model could be used in agro-ecosystem modelling applications to assess the

environmental impacts (such as surface ruoff and green-house gas emissions) of livestock-grazing systems and inform management strategies for ameliorating these.

1 Introduction

Soil compaction is a major environmental hazard. It is produced by stresses on or within the soil due to agricultural operations, usage of military, forestry and construction vehicles and animal treading under vulnerable soil conditions (Hamza and Anderson, 2005). Soil compaction adversely impacts soil mechanical and hydraulic properties (Keller et al., 2017, Rabot et al., 2018) and it is often linked with soil erosion (Nawaz et al., 2013), increased greenhouse gas (GHG) emissions (Oertel et al., 2016) and reduction of crop and pasture productivity (Håkansson and Reeder, 1994, Houlbrooke et al., 2009). These responses can have a strong effect on soil ecosystem services (Conrad, 1996, Aitkenhead et al., 2016, Foster et al., 2017) and economy (Graves et al., 2015).

Quantifying large scale environmental effects of soil compaction remains challenging due to fragmentary data on how soil processes and properties are affected by soil compaction across temporal and spatial scales. Early estimates by Oldeman (1992) suggested that 68 Mha of arable lands were compacted globally and recent estimates indicate that about 25-40% of all arable land is compacted in the United Kingdom (Graves et al., 2015), Denmark (Schjønning et al., 2015) and the Netherlands (Brus and Van Den Akker, 2018). Similarly, estimations by Steinfeld et al. (2006) suggest that 20% of the world's grasslands are degraded, mostly through overgrazing, compaction, and erosion caused by livestock treading.

Soil properties respond to soil compaction differently, presenting different relative post-compaction changes and recovery rates (Keller et al., 2021). Transport properties are often strongly reduced by compaction, diminishing the capacity of the soil to provide water and oxygen to plant roots due to a reduction and disruption of the soil pore system (primarily macropores), further leading to changes in soil evaporation (Assouline et al.,2014; Romero-Ruiz et al., 2022; Yi et al., 2022). In addition, the impact of compaction on soil mechanical properties limits the ability of plant roots to reach larger soil volumes and extract water (Bengough et al., 2011). All these interacting processes ultimately determine how water is partitioned through processes such as drainage, evaporation, root water uptake and surface runoff (Oades, 1993, Gregory et al., 2009, Or et al., 2021). Such limitations on water flow and gas diffusion can lead to anaerobic conditions favoured by the microorganisms responsible for denitrification (reduction of nitrate to produce nitric oxide, NO; nitrous oxide, N_2O; and nitrogen gas, N_2) in soil (Khalil et al., 2005). Our limited ability to qualitatively describe these processes is one barrier that constrains our understanding of environmental processes (e.g., water flow, carbon cycling, GHG emissions) from agriculture, especially in (but not limited to) livestock-grazing systems (Bilotta et al., 2007). Developing strategies for livestock-grassland management to ameliorate the animal's environmental impact will then largely rely on improving our qualitative and quantitative understanding of the underlying mechanisms affecting soil functioning at relevant spatial and temporal scales under real-world conditions. Integrative mechanistic modelling considering animal movement under different grazing strategies and how they modify key soil properties is currently lacking and may offer a crucial first step towards developing a more complete understanding of the environmental and economic consequences of soil degradation under grassland-livestock systems (Vereecken et al., 2016, Baveye et al., 2021).

The aim of this work is to develop a mechanistic model for predicting spatio-temporal changes of soil bulk density, porosity, macroporosity, and saturated hydraulic conductivity explicitly considering soil compaction due to animal grazing. Rates of natural soil recovery are also considered. To achieve this, we (1) developed a model of animal movement for a given soil area, (2) used a soil rheology model to calculate soil viscous deformation in response to animal treading, and (3) used the results from the rheology model along with commonly used soil physics models to calculate changes in soil properties in response to compaction. The modelling tool developed here was used to reproduce data from the literature showing changes in soil properties due to animal treading.

2 Soil compaction model

2.1 Soil structure: Conceptual model and definitions

In order to have a consistent representation of the various soil properties predicted by our soil compaction model (Figure 1) and to facilitate their computation, we first provide a definition of soil structure. This definition is used exclusively for this work, and may differ from other definitions found in the literature (Dexter, 1988). We consider the soil to be formed by two domains: (1) a soil matrix that is represented as an assembly of soil aggregates that encompass intra-aggregate porosity and (2) a soil macroporous region that can be conceptualized as inter-aggregate porosity (see Figures 2a, 2b and 2c). Similar conceptualizations have been successfully used to compute electrical (Day-Lewis et al., 2017, Romero-Ruiz et al., 2022), seismic (Dvorkin et al., 1999, Romero-Ruiz et al., 2021) and dielectric (Blonquist Jr et al., 2006) properties of structured porous media. Here, the total porosity (ϕ_T) is expressed as a function of the soil matrix porosity (ϕ_{sm}, pore radius r_p < 30 μm) and the macroporous region (ϕ_{mac} = 1, r_p > 30 μm) together with the volumetric fraction occupied by the soil macropores (w_{mac}) and the soil matrix (1 - w_{mac}):

$$\phi_T = (1 - w_{mac})\, \phi_{sm} + w_{mac}\phi_{mac}. \tag{1}$$

2.2 Bingham model of soil rheology applied to animal treading

For simplicity, the time-dependent signature stress applied on the soil by a walking animal (Scholefield and Hall, 1986) is represented here by a half-sine cycle. This is similar to the more widely used representation of the transient stress produced by the passage of vehicles (Or and Ghezzehei, 2002). Moreover, this simple representation allows modelling soil deformation due to animal treading using the Bingham rheology model (Ghezzehei and Or, 2001). The application of a transient load by a walking animal will then result in an elastic (temporary) and a viscous (permanent) deformation of the soil frame producing an axial strain $\epsilon = \epsilon_e + \epsilon_v$ (see Figure 2, Ghezzehei and Or, 2003), where ϵ_e and ϵ_v are the elastic and viscous strains, respectively. The lasting effect of one treading event produces an irreversible deformation, ϵ_v, which can be modelled using information about the initial (prior to compaction) strain ϵ_0, the axial load and duration of stress application and the soil rheological properties as:

$$\epsilon_v(t) = \left[\epsilon_B^2 S_{sm}(t)^{N_\mathrm{v}} \left(1 - cos(\omega t)\right) + \epsilon_0^2\right]^{\frac{1}{2}}, \tag{2}$$

where t is the time, ω is the angular frequency, ϵ_B comprises information of the soil rheological properties and the characteristics of the compaction event (e.g., weight of animal and walking speed), $S_{sm} = \theta_{sm}/\phi_{sm}$ is the water saturation in the soil matrix, where θ_{sm} is the water content in the soil matrix and N_v is an empirical exponent. Note that deformation is assumed to occur in aggregate contacts forming the soil matrix; equation 2 thus takes the properties and states of the soil matrix.

The extent of soil compaction damage produced by animal treading is strongly dependent on soil water content. As described by Drewry et al., (2008), the main effects of water content-dependent soil responses to treading are: (i) little soil compaction damage and elastic recovery for treading events when soil water contents are low, (ii) viscous deformation and greater soil compaction damage for higher soil water contents (e.g., in the vicinity of field capacity) and (iii) high risk of pugging for water contents near full water saturation. The effects (i) and (ii) are accounted for in Equation 2, where the product $\epsilon_B^2 S_{sm}(t)^{N_\mathrm{v}}$ is a function of the soil complex viscosity (Vyalov, 1986). For simplicity, we propose using the time- and water content-dependent term $S_{sm}(t)^{N_\mathrm{v}} = (\theta_{sm}(t)/\phi_{sm})^{N_\mathrm{v}}$ for modelling the effect of water saturation on the complex viscosity and resulting viscous strain. This function is similar to other models of soil properties, for example, accounting for effects of water saturation in soil electrical resistivity (Archie, 1980) or the effective stress parameter (Nuth and Laloui, 2008) for calculating suction stresses. The viscous strain ϵ_v can thus be used to model soil properties by means of geometrical approximations as shown in the following sections. Similarly, ϵ_v for transient loads (i.e., a walking animal or a passing vehicle), can be derived from an expression for viscous strain for static loads. However, for simplicity, in this study we only focus on transient loads (equation 2).

2.3 Spatio-temporal evolution of compaction patterns

We incorporate spatial and temporal dynamics of compaction patterns by simulating animal movement within a defined area that is further discretized in cells. For simplicity, a random walk algorithm is used to simulate animal movement within the delimited area by setting the stock density (*D*) and the number of steps per day per animal (N_{steps}). We then count the number of steps per day per cell, simulating full spatial dynamics of animal movement in a field. To translate this information to soil deformation, Equation 2 is used recursively making a daily update of the strain associated with each cell. This process can be further constrained using GPS data from animals.

2.4 Bulk density, total porosity and microporosity

Having the strain as a function of time and assuming deformation in all axes, as proposed by Ghezzehei and Or (2001), we can calculate the bulk density of compacted soils (ρ_c) as a function of the compacted strain (ϵ_c), the initial strain (ϵ_0), and the initial bulk density (ρ_0) as:

$$\rho_c = \rho_0 \left(\frac{1-\epsilon_0}{1-\epsilon_c}\right)^3.$$

3

Similarly, the total porosity (ϕ_{T_c}) can be calculated as:

$$\phi_{T_c} = 1 - \frac{\rho_c}{\rho_p},$$

4

where ρ_p is the bulk density of soil particles ($\sim$ 2.7 g/cm^3). It has been extensively shown that soil compaction impacts primarily soil macroporosity while the microporous domain remains largely unaffected (see Or and Ghezzehei, 2002, Berli et al., 2008). For this reason, we attribute changes in total porosity due to compaction completely. Reductions of macroporosity after a treading event are calculated as (for $\Delta\phi_T > 0$):

$$\Delta w_{mac} = \Delta\phi_T,$$

$$w_{mac_c} = w_{mac_0} - \Delta\phi_T,$$

5

where w_{mac}, w_{mac_c}, and w_{mac_0} are macroporosity, macroporosity after compaction and initial macroporosity, respectively.

2.5 Water retention and hydraulic properties

We account for soil structure and macropore water flow using the water retention and hydraulic model proposed by Durner (1994). This model is consistent with our conceptual description of soil structure dividing the soil porosity into two overlapping domains representing (1) the pore system in the soil matrix and (2) the macropore system. In this parametrization, the water retention and the hydraulic conductivity function of the soil are expressed as a combination of the functions ascribed to the two considered domains:

$$S_e = \frac{\theta - \theta_r}{\phi_T - \theta_r} = w_{sm}[1 + (\alpha_{sm} h)^{n_{sm}}]^{1-\frac{1}{n_{sm}}} + w_{mac}[1 + (\alpha_{mac} h)^{n_{mac}}]^{1-\frac{1}{n_{mac}}},$$

6

and

$$K_{soil} = r_k K_{sm} \frac{\left(w_{sm} S_{e_{sm}} + w_{mac} S_{e_{mac}}\right)^{0.5}}{(w_{sm}\alpha_{sm} + w_{mac}\alpha_{mac})^2} \left(w_{sm}\alpha_{sm} \left[1 - \left(1 - S_{e_{sm}}^{\frac{n_{sm}}{n_{sm}-1}} \right)^{1-\frac{1}{n_{sm}}} \right] + w_{mac}\alpha_{mac} \left[1 - \left(1 - S_{e_{mac}}^{\frac{n_{mac}}{n_{mac}-1}} \right)^{1-\frac{1}{n_{mac}}} \right] \right)^2,$$

7

where h is the pressure head, S_e is the effective saturation of the soil, θ_r is the residual water content, n_i is the van Genuchten exponent (which is related to soil texture) and α_i is related to the inverse of the air-entry pressure. The saturated hydraulic conductivity of the soil $K_{sat} = r_k K_{sm}$ is defined as the product of the saturated hydraulic conductivity of the soil matrix K_{sm} and the ratio $r_k = K_{sat}/K_{sm}$ which is a function of the soil macroporosity. The indices *sm* and *mac* represent the soil matrix and the macroporous region, respectively. Equation 7 is used to calculate the hydraulic conductivity as a function of water content (or pressure head). Such parametrization can be approximated by a linear combination of the hydraulic conductivity functions of the two domains as (see Fatichi et al., 2020, Romero-Ruiz et al., 2022):

$$K_{soil}(h,z) = \left(1 - w_{mac_c}(z)\right)K_{matrix}(h,z) + w_{mac_c}(z)K_{macropore}(h,z),$$

8

where *z* is the vertical spatial coordinate. This allows representing the K_{sat} as a function of the macroporosity w_{mac}. Thus, a reduction of saturated hydraulic conductivity can be calculated using equation 8 and updating the compaction induced change in w_{mac} resulting from equation 5 as:

$$K_{sat_c}(z) = \left(1 - w_{mac_c}(z)\right)K_{matrix_{sat}}(z) + w_{mac_c}(z)K_{macropore_{sat}}(z).$$

9

Equation 9 is simplified and implies that changes in unsaturated flow (occurring in the soil matrix) is the same for compacted and non-compacted soils (Fatichi et al., 2020) which may not be always the case (Berli et al., 2008). Where macroporosity is absent (e.g., in non-structured soils or where compaction has removed macroporosity), the saturated hydraulic conductivity can be calculated using the expression proposed by Or et al. (2000) based on the Kozeny-Carman relationship:

$$K_{sat_c} = K_{sat_0} \frac{\phi_{T_c}\left(1 - \phi_{T_0}\right)^2}{\phi_{T_0}\left(1 - \phi_{T_c}\right)^2},$$

10

where the K_{sat_0} is the initial saturated hydraulic conductivity (i.e., non-compacted). If necessary, vertical changes of saturated hydraulic conductivity of the soil K_{sat} can be approximated with a function that decays exponentially with soil depth, similarly to decay of soil organic matter and macroporosity with depth (Araya and Ghezzehei, 2019, Kramer and Gleixner, 2008, Hobley and Wilson, 2016).

2.6 Soil structure recovery

It is expected that soil macro and micro-porosities change dynamically as a function of time in response to biological activity (earthworm movement and root decay), seasonal climatic cycles and management. Meurer et al. (2020) showed that macroporosity (w_{mac}) recovers at an exponential rate asymptotically to a maximum macroporosity (w_{mac_0}). Similarly, we empirically account for soil structure recovery in the viscous strain as:

$$\epsilon_v = \epsilon_0 - (\epsilon_0 - \epsilon_i)e^{-d_r/\lambda_{tr}},$$

11

where ϵ_i is the soil strain, representing the strain resulting after the grazing season, d_r is the number of days after the last grazing season, and λ_{tr} determines the recovery rate. In this work, we did not consider recovery by wetting and drying cycles. However, the model by Stewart et al. (2016) could be used to predict changes in soil porosity resulting from swelling events.The changes in pore-spaces described in this section generate soil structure recovery and produce concurrent changes in soil bulk density and saturated hydraulic conductivity which are updated using the models described in the previous section.

3 Case study: Tussock Creek, New Zealand

3.1 Soil compaction experiment

We make use of data from the Tussock Creek experimental platform (-46.2 N, 168.4 E) in New Zealand reported by Houlbrooke et al. (2009). The soil (Pukemutu silt loam) has a texture of 32% clay (< 2 μm), 65% silt (2-60 μm), and 3% sand (60-2000 μm). Pasture at the experimental site was predominantly a mix of ryegrass (Lolium perenne L.) and white cover (Trifolium repens L.). Soil fertility levels were optimal for pasture production, with pH at 5.9, Olsen P at 40 μg/ml, sulphate-S at 6.6 $\mu g/g$ and organic carbon content of 4.5%. This study investigated the ability of grazing practices to prevent soil degradation by livestock treading. As per common practice for the region, the site was rotationally grazed (stocking density of 65 animals/ha) on 10 – 12 occasions throughout spring, summer and autumn and remained ungrazed over winter. Specific treatments were: (1) normal (rotational) grazing of undrained land, (2) normal grazing, (3) normal grazing then restricted to 3-hour grazing periods during autumn, (4) normal grazing, but restricted to 3 hours grazing when the soil was wet, (5) strategic grazing to avoid soil pugging damage when conditions were wet, and (6) never grazed. With the exception of treatment 1, treatment plots were artificially drained by a mole-pipe drainage system, as is common practice for the naturally poorly drained Pokemutu soil. Grazing scheduling for treatments 4 and 5 was guided by the use of a cone penetrometer; further details can be found in Houlbrooke et al. (2009). Treatment responses were observed using measurements of bulk density, macroporosity and saturated hydraulic conductivity for the 0-5 cm soil layer at the end of winter and spring in three consecutive years from 2000 to 2002. These sampling times were scheduled to coincide with occasions when soil physical condition was expected to reflect winter recovery or maximum damage due to cow treading during spring, respectively. Grazing periods, water contents and temperatures at the Tussock Creek experimental station are presented in Figure 3.

3.2 Modelling considerations

We aimed to systematically capture and reproduce primary signatures of soil compaction due to animal treading in key soil properties and how they recover after the grazing season. For this, we set the model to reproduce the soil compaction experiment by Houlbrooke et al. (2009). For all treatments, there was a drop in macroporosity during the spring grazing season followed by a period of significant recovery (returning to pre-grazing conditions in most cases; see averaged macroporosities in Figure 4). As discussed by the authors, the grazing strategies that were used to prevent structural damage within the top 10 cm of the soil were not strikingly different to conventional grazing practices (see statistical analysis in Houlbrooke et al., 2009). For this reason, we compared two basic treatments: (1) grazed vs (2) non-grazed. Data from the nil grazed treatments were used for non-grazed. Grazed treatment data were obtained by averaging measurements from all the grazing treatments described in section 3.1. As shown in Figure 4, we used data from the first two grazing seasons (2000 and 2001) to calibrate key model properties (data used for inverse modelling, data I) and evaluated the ability of the model to predict data from the third grazing season (2002) (data predicted for validation, data P). The calibrated properties were: ϵ_B containing information about the compaction event, the initial bulk density ρ_0, the rate of recovery λ_{tr}, the porosity of the soil matrix ϕ_{sm}, the hydraulic conductivity of the soil matrix K_{sm} and the exponent N_ν.

For simplicity, we assumed that compaction occurred during spring and recovery occurred in all other seasons (see also Drewry et al., 2004). To simulate the treading events, we did not report the spatial variation of soil properties but instead focused on the median value for each treatment and its temporal variations utilizing a daily time step in the model. We simulated random animal movement in a 100 x 100 m square field using the characteristics of the grazing experiments (about 12 grazing days per season using c. 65 cows per hectare on each occasion), considering information about the grazing dates (Figure 3a) and assuming 5000 steps per animal per day. We then selected the median of the numbers of steps counted per cell (see Figure 5) to be representative of the treading event. This resulted in 97 steps per grazing day. For each of the grazing days, Equation 2 is then used recursively 97 times to obtain the associated compaction-induced viscous strain. We considered that soil structure recovery is dominated by bioturbation. The recovery of soil strain was simulated outside spring using Equation 11. Bulk density, macroporosity and saturated hydraulic conductivity were then updated daily using equations 3-5 and 7-8 reflecting changes induced by compaction and recovery agents. We used the three data sets of Houlbrooke et al. (2009) (bulk densities, macroporosities and saturated hydraulic conductivities) for inverting the key model properties representing compaction and recovery. Such model properties ($\boldsymbol{P} = [\epsilon_B, \lambda_{tr}, \rho_0, \phi_{sm}, K_{sm}, N^{\nu}]$) are inferred using the Markov-chain Monte Carlo (MCMC) method of Laloy and Vrugt (2012) (the so-called differential evolution adaptive Metropolis, DREAM(ZS)). The posterior probability density functions of the model properties were inferred using the following likelihood function:

$$L(\boldsymbol{P}|\boldsymbol{d}\} = \left(\sqrt{2\pi\sigma_{\boldsymbol{d}}}\right)^{-N_d} exp\left[-\frac{1}{2}\sum_{d_{i=1}}^{Nd}\left(\frac{F_i(\boldsymbol{P}) - d_i}{\sigma_{d_i}}\right)^2\right],$$

11

where F(**P**) and **d** are the simulated and measured data (simultaneously containing bulk densities, macroporosities and saturated hydraulic conductivities), respectively, σ_{d_i} is the data error of the i-th datum (considered here as 5% of each datum) and N_d is the number of data points. We used uniform probability distributions as priors of all inverted properties.

4 Results

After burn-in for 10000 iterations, the mean values inferred from the posterior distributions were ϵ_B= 0.31%, λ_{tr}= 52.17 days, ρ_0= 0.91 g/cm^3, K_{sm}= 0.04 cm/h and $N_\nu = 3.44$. The model succeeded in reproducing the data used for inversion (first two grazing seasons) resulting in a weighted root-mean square error (WRMSE) of 1.25. A reasonable fit was obtained for data not included in the inversion (third grazing season) with a WRMSE of 2.8. For the grazed treatment the bulk density increased as a result of grazing, but then recovered to a level similar to pre-grazing (Figure 6a). The bulk density of the non-grazed treatment was variable: increasing on occasions during the spring and decreasing during the summer, fall and winter seasons. The bulk density of the non-grazed treatment was less for all measurement occasions after the first grazing season. The final bulk density of the grazed treatments was 14% higher than in the non-grazed treatment. The post-spring grazing bulk density was 27% higher than the pre-grazing bulk density for the last grazing season.

We present (Figure 6a) the modelled bulk densities as a function of time resulting from the MCMC inversion considering chains after 10000 iterations. The modelled bulk densities reflect changes due to compaction and recovery and reproduced the patterns of the observed bulk densities from the first two grazing seasons reasonably well. The bulk densities corresponding to the third grazing season, not considered in the inverted data vector, were slightly overestimated by the model. This can be partly explained bythe considerably lower values of bulk density measured in 2002 compared to values from 2000 and 2001. Similar to the bulk density measurements, the saturated hydraulic conductivity decreased in response to compaction during spring grazing periods and increased during the recovery periods (Figures 6c). We observed typically higher values in the non-grazed treatment. However, the variations in saturated hydraulic conductivities were substantially larger when comparing grazed vs non-grazed treatments (78% drop at the last measurement occasion) and pre- vs post-grazing (95% drop at the last ocassion). Despite such large variations, the model provided a reasonable description of compaction and recovery cycles and captured measured values quantitatively. By considering a dual-domain conceptual model of soils that explicitly takes account of the effects of macropores on soil hydraulic properties, it is possible to simultaneously reproduce large changes in hydraulic properties alongside relatively small changes in bulk density (see Figure 7a).

Saturated hydraulic conductivity (Figure 6c) was strongly dependent on soil macroporosity (see Figure 7b) and thus followed similar trends (refer to Figures 6b and 6c). The final macroporosity was 45% less for the grazed than for the non-grazed treatments. As seen for the bulk density and macroporosity data (Figures 6a and 6b) changes induced during the spring 2001 were less marked than those induced in the springs of 2000 and 2002. By considering the effects of water saturation on the potential damage to soil compaction (Equation 2), this effect was reasonably well reproduced by the model that predicts a smaller impact on soil properties for the drier spring of 2001 compared to the wetter springs of 2000 and 2002. Overall, the macroporosity data and tendencies responding to compaction and recovery are reasonably well reproduced by the model for both data I and data P.

5 Discussion

The modelling framework presented in this work predicts compaction-induced changes in soil properties due to animal treading. We intentionally only sought to represent primary features of soil compaction in order to provide a model that is relatively easy to implement and helps assessing impacts of management on soil properties and functions. As demonstrated in the Results section, the model does a reasonable job of reproducing not only data from grazing seasons in 2000 and 2001 (i.e., those used for property calibration), but also for data from grazing in 2002. However, it is important to stress that changes in soil properties and functions due to compaction are very complex and some limitations in the model remain as described below.

The model uses a very simple approach to calculate bulk densities, macroporosities and saturated hydraulic conductivities (equations 3, 5, 7 and 9). Despite this simplicity, the macroporosity and saturated hydraulic conductivity data were particularly well reproduced. This is partly explained by the ability of the model to represent the dependency of saturated hydraulic conductivity on macroporosity (Figure 7), employing a linear superposition of the two porosity domains using Equations 7 and 10. Such larger variations are difficult to capture when using more common approaches that obviate macroporosity effects (e.g., Equation 11). The variability in bulk density in response to compaction is much less, but is consistent with values observed in the literature of about 15% decrease (Keller et al., 2017). The model was able to reproduce variations in bulk density successfully, but bulk densities from the non-grazed treatment did not show a clear baseline (i.e., a constant value as a function of time) characteristic of non-grazed soils. In contrast, we did observe a less variable baseline for macroporosity and saturated hydraulic conductivity values in the non-grazed treatment. These variations in baselines may be attributed to the natural spatial variability of soil properties in grasslands and, for simplicity, possible effects related to them (e.g., swelling-induced compaction) were not considered in the model. Having a highly variable baseline of bulk density and a less variable baseline for macroporosity is to be expected if we acknowledge that bulk soil properties such as bulk density and total porosity only offer an incomplete representation of soil structure (Romero-Ruiz et al., 2018, Rabot et al., 2018, Or et al., 2021). As shown in Figure 7, this means that saturated hydraulic conductivity, which is a property that is more representative of soil structure, can vary substantially for the same value of porosity (or bulk density) in response to redistributions of pore sizes and connectivities, such as those resulting from compaction and shear deformation (Whalley et al., 2012) which were not explicitly considered in this study.

The model considers porosity (ϕ_{sm}) and hydraulic conductivity of the soil matrix (K_{sm}) to be constant as function of time. This assumption was based on evidence suggesting that soil compaction primarily impacts inter-aggregate pore spaces (macropores) and aggregate contacts (Berli et al., 2008; Eggers et al., 2006; Ghezzehei & Or, 2001). However, other studies have shown that soil compaction may increase both the porosity of the soil matrix and the unsaturated hydraulic conductivity due to redistributions of pore spaces and their connectivity (Richard et al., 2001). If necessary, such changes can be incorporated in the water saturation and hydraulic conductivity functions (equations 6 and 7). Similarly, we did not consider changes in pore connectivity of the macroporous region which has been demonstrated to have a large influence on soil hydraulic properties (e.g., Fu et al., 2020; Müller et al., 2018). This may help explain some of the mismatch between measured and modelled hydraulic conductivities and macroporosities presented in Figure 7b.

We modelled three grazing periods considering the dates of grazing (Figure 3a), the stock density (65 animals per hectare) and the water content measured on the grazing dates (Figure 3a). The strain ϵ_B (which helps determining the susceptibility of the soil to compaction) was set constant in space and time in the model, reflecting that all soil compaction events (i.e., animal trampling) occurred under the same soil texture and animal weight. We proposed to model the susceptibility to compaction as a function of the water content by using the term S^{N_ν} in Equation 2. This function has the ability of assigning a dependency of the soil compaction damage with the corresponding soil wetness conditions during the compaction event. It is difficult and outside the scope of this work to properly determine the parameter ϵ_B and function S^{N_ν} as a function of time and for different soil textures. They mainly depend on: Poisson's ratio and complex viscosity of the soil, the hoof pressure and velocity of the walking animals and the size of aggregates conceptualized as forming the soil (Ghezzehei and Or, 2001). For practical reasons, we opted for calibrating only ϵ_B and N_ν. Despite lacking a complete explicit consideration of the various soil physical properties, environmental conditions and characteristics of the compacting stresses, the model remains valid and could be further used for comparing different grazing strategies (e.g., involving livestock animals with different weights such as sheep). Moreover, the model simultaneously reproduced compaction-induced variations of some soil physical properties. The model predicted changes in soil properties to be larger during the springs of 2000 and 2002 than changes in properties after the drier spring of 2001 (see Figures 6b and 6c). The predicted compaction-induced reductions in macroporosity during the spring were 65%, 46%, and 80% for 2000, 2001, and 2002, respectively; corresponding measured reductions were 53%, 46%, and 80%, respectively. Similarly, the model predicted saturated hydraulic conductivity reductions of 90%, 76%, and 96% for 2000, 2001, and 2002, respectively; which were consistent with their corresponding measured reductions (compared with the non-grazed control treatment) of 93%, 62%, and 95%. The data confirmed that soil water content largely controls the susceptibility of the soil to compaction (see discussions by Drewry et al., 2008) and the results suggested that the representation of water content effects in the model is sufficient to capture such influence. Further field and laboratory research may be performed to explicitly determine ϵ_B and the function S^{N_v}. This includes applying the modelling framework presented here to other data-sets, for soil with different textures, different grazing histories and under different climate.

Similar to the compaction process, we opted for using a simplified representation of soil recovery (Equation 11). This model simulated the evolution of soil pore-spaces only in response to bioturbation by decaying roots and earthworms (Meurer et al.,2020). Effects of climatic cycles such as wetting-drying and freezing-thawing have been suggested as important factors playing a role in soil structure evolution and recovery (Kuan et al., 2007, Gregory et al., 2007). We did not observe major wetting-drying events nor indications of soil freezing in the water content and temperature data presented in Figure 3. For this reason, these processes were not considered. The recovery property $\lambda_{tr}$was constant with time and the same for both recovery periods. It is therefore expected that some data might be mis-predicted. The model predicts a rapid recovery after the grazing periods which is consistent with the compaction and recovery cycles observed by Drewry et al. (2004). This was difficult to validate, however, due to the small number of data points measured as a function of time. Future campaigns dedicated to the study of soil structure recovery may benefit from having more frequent monitoring of soil properties shortly after compaction.

We inferred a mean value for λ_{tr} of approximately 52 days, indicating that the soil properties recover about one third of the relative change during this period. Regardless of the mechanisms responsible for soil recovery, data presented by Houlbrooke et al. (2009) and modelled in this work presented an atypically rapid recovery rate for the 0-10 cm soil depth.

Soil compaction is often regarded as a process involving very slow recovery rates, yet there is still some discrepancy in the recovery rates that are site-specific and may dramatically vary ranging from months to decades depending on soil texture, soil cover, soil depth, management history, and local climate conditions (Berisso et al., 2012; Schjonning et al., 2013; Keller et al., 2021).

Despite offering a relatively broad description of the processes involved in soil structure dynamics, several simplifications were made in the model. The model does not considers variations of soil properties with soil depth. This is a reasonable choice for modelling compaction by animal treading, that mainly affects soil properties of the topsoil (Leitinger et al., 2010). However, if modelling soil compaction by the passage of heavy agricultural machinery, stress propagation in the soil profile may be considered to fully capture variations of soil properties (Keller et al., 2013, Ghezzehei and Or, 2003). Similarly, soil structure recovery is modelled by only using an exponential function asymptotically approaching a limiting value of a given property (Meurer et al., 2020). Future modelling work may deal with assessing recovery as a function of depth by, for example, proposing a depth-dependent function for λ_{tr}. In addition, we did not consider shear deformation which may be important when compacting stresses occur under very wet conditions (Whalley et al., 2012).

The model presented in this work describes the impact of compaction by animal treading on soil properties that in turn affect soil-water and -nutrient flows. The dynamics of these processes are commonly incorporated into agroecosystems models (Coleman et al., 2017; Wu et al., 2007; Dondini et al., 2017). The relative simplicity of our model means that, provided that properties can be measured or calibrated (ϵ_B and N_ν), it can be readily incorporated into such modelling systems, allowing them to then describe the impact of livestock management (i.e., stocking rate and length of grazing) on processes involving soil water dynamics, such infiltration, water flow, evaporation, drainage (Romero-Ruiz et al., 2022) and their consequences for the environment (e.g., in GHG emissions) and production. The model may therefore be valuable for informing management strategies for the mitigation of nutrient losses and emissions.

6 Conclusions

By considering a physically based model of soil deformation due to compaction, the modelling framework presented here can systematically incorporate important elements related to soil management practices in grasslands for evaluation of their impact on soil properties. The model captures the main effects of soil compaction on key soil properties, it is simple and it is relatively easy to implement. It does not explicitly take into account some of the more complex effects that soil compaction has on the soil pore system and hydraulic functions, such as changes to pore continuity. We tested the model using data from a grazing experiment at the Tussock Creek experimental platform in New Zealand. Our model successfully reproduced bulk density, macroporosity and saturated hydraulic conductivity data. By fitting the data with model properties associated with the soil's susceptibility to compaction and ability to recover, the model confirmed that drier soils are less prone to compaction and that the overall damage is less in drier years. In addition, as suggested by the seasonally collected data, the model predicted a rapid recovery after the grazing seasons. This indicates that future campaigns focusing on monitoring recovery should consider high frequency monitoring for periods shortly after compaction events. The model presented here is limited by our ability to measure or calibrate its parameters, yet, if this is achieved, it offers a tool for qualitative and quantitative assessment of different grazing management strategies by predicting their impact on key soil properties. The model improves our understanding of the impact of management factors on soil states and processes and thus may have utility for predicting the wider environmental impacts of soil compaction, such as water flow, carbon cycling and greenhouse gas emissions.

Acknowledgments

Rothamsted Research receives grant aided support from the Biotechnology and Biological Sciences Research Council (BBSRC) of the United Kingdom. This research was supported by the Biotechnology and Biological Sciences Research Council (BBSRC) Institute Strategic Programme (ISP) grants, “Soils to Nutrition” (S2N) grant numbers BBS/E/C/000I0320 and BBS/E/C/000I0330. The authors thank two anonymous reviewers for their insightful comments that helped to improve the quality of this manuscript.

References

Aitkenhead, M., S. D. Allison, S. Assouline, P. Baveye, M. Berli, N. Brüggemann, P. Finke, M. Flury, T. Gaiser, G. Govers, T. Ghezzehei, P. Hallett, H. J. H. Franssen, J. Heppell, R. Horn, J. A. Huisman, D. Jacques, F. Jonard, S. Kollet, F. Lafolie, K. Lamorski, D. Leitner, A. Mcbratney, B. Minasny, C. Montzka, W. Nowak, Y. Pachepsky, J. Padarian, N. Romano, K. Roth, Y. Rothfuss, E. C. Rowe, A. Schwen, J. ŠimÅ´rnek, A. Tiktak, J. V. Dam, S. E. A. T. M. V. D. Zee, H. J. Vogel, and J. A. Vrugt (2016), Modelling Soil Processes: Review, Key Challenges, and New Perspectives Brief History of Soil Modelling, Vadose Zone Journal, 15, doi:10.2136/vzj2015.09.0131.

Araya, S. N., and T. A. Ghezzehei (2019), Using machine learning for prediction of saturated hydraulic conductivity and its sensitivity to soil structural perturbations, Water Resources Research, 55(7), 5715–5737, doi:https://doi.org/10.1029/2018WR024357.

Assouline, S., K. Narkis, R. Gherabli, P. Lefort, and M. Prat (2014), Analysis of the impact of surface layer properties on evaporation from porous systems using column experiments and modified definition of characteristic length, Water Resources Research, 50(5), 3933–3955, doi:10.1002/2013WR014489.

Baveye, P. C., E. Dominati, A. Grêt-Regamey, and H.-J. Vogel (2021), Assessment and modelling of soil functions or soil-based ecosystem services: Theory and applications to practical problems, Frontiers in Environmental Science, p. 549.
Bengough, A. G., B. M. McKenzie, P. D. Hallett, and T. A. Valentine (2011), Root elongation, water stress, and mechanical impedance: a review of limiting stresses and beneficial root tip traits, Journal of Experimental Botany, 62(1), 59–68, doi:10.1093/jxb/erq350.

Berisso, F. E., et al. "Persistent effects of subsoil compaction on pore size distribution and gas transport in a loamy soil." Soil and Tillage Research 122 (2012): 42-51. https://doi.org/10.1016/j.still.2012.02.005

Berli, M., A. Carminati, T. A. Ghezzehei, and D. Or (2008), Evolution of unsaturated hydraulic conductivity of aggregated soils due to compressive forces, Water Resources Research, 44(5), doi:https://doi.org/10.1029/2007WR006501.

Bilotta, G., R. Brazier, and P. Haygarth (2007), The impacts of grazing animals on the quality of soils, vegetation, and surface waters in intensively managed grasslands, pp. 237–280, Academic Press, doi:https://doi.org/10.1016/S0065-2113(06)94006-1.

Blonquist Jr, J., S. B. Jones, I. Lebron, and D. Robinson (2006), Microstructural and phase configurational effects determining water content: Dielectric relationships of aggregated porous media, Water Resources Research, 42(5), doi:10.1029/2005WR004418.

Brus, D. J., and J. J. Van Den Akker (2018), How serious a problem is subsoil compaction in the Netherlands? A survey based on probability sampling, Soil, 4(1), 37–45, doi:10.5194/soil-4-37-2018.

Coleman, K., S. E. Muhammed, A. E. Milne, L. C. Todman, A. G. Dailey, M. J. Glendining, and A. P. Whitmore (2017), The landscape model: A model for exploring trade-offs between agricultural production and the environment, Science of The Total Environment, 609, 1483–1499, doi:https://doi.org/10.1016/j.scitotenv.2017.07.193.

Conrad, R. (1996), Soil microorganisms as controllers of atmospheric trace gases (h2, co, ch4, ocs, n2o, and no)., Microbiology and Molecular Biology Reviews, 60(4), 609–640.

Day-Lewis, F., N. Linde, R. Haggerty, K. Singha, and M. A. Briggs (2017), Pore network modelling of the electrical signature of solute transport in dual-domain media, Geophysical Research Letters, 44(10), 4908–4916, doi:10.1002/2017GL073326.

Dexter, A. (1988), Advances in characterization of soil structure, Soil and Tillage Research, 11(3-4), 199–238, doi:10.1016/0167-1987(88)90002-5.

Dondini, M., Richards, M., Pogson, M., Jones, E.O., Rowe, R.L., Keith, A.M., McNamara, N.P., Smith, J.U. and Smith, P. (2016), Evaluation of the ECOSSE model for simulating soil organic carbon under *Miscanthus* and short rotation coppice-willow crops in Britain. GCB Bioenergy, 8: 790-804. https://doi.org/10.1111/gcbb.12286

Durner, W. (1994), Hydraulic conductivity estimation for soils with heterogeneous pore structure, Water Resources Research, 30(2), 211–223, doi:10.1029/93WR02676.

Drewry, J. J., Paton, R. J., & Monaghan, R. M. (2004). Soil compaction and recovery cycle on a Southland dairy farm: implications for soil monitoring. Soil Research, 42(7), 851-856.

Drewry, J. J., Cameron, K. C., & Buchan, G. D. (2008). Pasture yield and soil physical property responses to soil compaction from treading and grazing—a review. Soil Research, 46(3), 237-256.

Dvorkin, J., M. Prasad, A. Sakai, and D. Lavoie (1999), Elasticity of marine sediments: Rock physics modelling, Geophysical Research Letters, 26(12), 1781–1784, doi:10.1029/1999GL900332.

Fatichi, S., D. Or, R. Walko, H. Vereecken, M. H. Young, T. A. Ghezzehei, T. Hengl, S. Kollet, N. Agam, and R. Avissar (2020), Soil structure is an important omission in Earth System Models, Nature Communications, 11(1), 1–11, doi:10.1038/s41467-020-14411-z.

Foster, T., N. Brozovic, and A. P. Butler (2017), Effects of initial aquifer conditions on economic benefits from groundwater conservation, Water Resources Research, 53(1), 744–762, doi:https://doi.org/10.1002/2016WR019365.

Fu, Z., Hu, W., Beare, M., Thomas, S., Carrick, S., Dando, J., Langer, S., Müller, K., Baird, D. and Lilburne, L., 2021. Land use effects on soil hydraulic properties and the contribution of soil organic carbon. Journal of Hydrology, 602, p.126741.

Ghezzehei, T. A., and D. Or (2001), Rheological properties of wet soils and clays under steady and oscillatory stresses, Soil Science Society of America Journal, 65(3), 624–637, doi:10.2136/sssaj2001.653624x.

Ghezzehei, T. A., and D. Or (2003), Stress-induced volume reduction of isolated pores in wet soil, Water Resources Research, 39(3), doi:10.1029/2001WR001137.

Graves, A., J. Morris, L. Deeks, R. Rickson, M. Kibblewhite, J. Harris, T. Farewell, and I. Truckle (2015), The total costs of soil degradation in England and Wales, Ecological Economics, 119, 399–413, doi:10.1016/j.ecolecon.2015.07.026.

Gregory, A., C. Watts,W. Whalley, H. Kuan, B. Griffiths, P. Hallett, and A. Whitmore (2007), Physical resilience of soil to field compaction and the interactions with plant growth and microbial community structure, European Journal of Soil Science, 58(6), 1221–1232.

Gregory, A. S., C. W. Watts, B. S. Griffiths, P. D. Hallett, H. L. Kuan, and A. P. Whitmore (2009), The effect of long-term soil management on the physical and biological resilience of a range of arable and grassland soils in england, Geoderma, 153(1-2), 172–185.

Håkansson, I., and R. C. Reeder (1994), Subsoil compaction by vehicles with high axle load, persistence and crop response, Soil and Tillage Research, 29(2), 277–304, doi:10.1016/0167-1987(94)90065-5.

Hamza, M. A., and W. K. Anderson (2005), Soil compaction in cropping systems: A review of the nature, causes and possible solutions, Soil and Tillage Research, 82(2), 121–145, doi:10.1016/j.still.2004.08.009.

Hobley, E. U., and B. Wilson (2016), The depth distribution of organic carbon in the soils of eastern Australia, Ecosphere, 7(1), climate, conditional inference trees, cropping, datamining, gradient boosting machines, grazing, land use, machine learning, randomForests, doi:10.1002/ecs2.1214, e01214.

Houlbrooke, D., J. Drewry, R. Monaghan, R. Paton, L. Smith, and R. Littlejohn (2009), Grazing strategies to protect soil physical properties and maximise pasture yield on a southland dairy farm, New Zealand Journal of Agricultural Research, 52(3), 323–336.

Keller, T., M. Carizzoni, F. E. Berisso, M. Stettler, and M. Lamandé (2013), Measuring the dynamic soil response during repeated wheeling using seismic methods, Vadose Zone Journal, 12(3), 8830, doi:10.2136/vzj2013.01.0033.

Keller, T., T. Colombi, S. Ruiz, M. P. Manalili, J. Rek, V. Stadelmann, H. Wunderli, D. Breitenstein, R. Reiser, H. Oberholzer, S. Schymanski, A. Romero-Ruiz, N. Linde, P. Weisskopf, A. Walter, and D. Or (2017), Long-term Soil Structure Observatory for monitoring post-compaction evolution of soil structure, Vadose Zone Journal, 16(4), doi:10.2136/vzj2016.11.0118.

Keller, T., T. Colombi, S. Ruiz, S. J. Schymanski, P. Weisskopf, J. Koestel, M. Sommer, V. Stadelmann, D. Breitenstein, N. Kirchgessner, A. Walter, and D. Or (2021), Soil structure recovery following compaction: Short-term evolution of soil physical properties in a loamy soil, Soil Science Society of America Journal, 85(4), 1002–1020, doi:https://doi.org/10.1002/saj2.20240.

Khalil, K., P. Renault, and B. Mary (2005), Effects of transient anaerobic conditions in the presence of acetylene on subsequent aerobic respiration and n2o emission by soil aggregates, Soil Biology and Biochemistry, 37(7), 1333–1342.

Kramer, C., and G. Gleixner (2008), Soil organic matter in soil depth profiles: Distinct carbon preferences of microbial groups during carbon transformation, Soil Biology and Biochemistry, 40(2), 425 – 433, doi:10.1016/j.soilbio.2007.09.016.

Kuan, H., P. Hallett, B. Griffiths, A. Gregory, C. Watts, and A. Whitmore (2007), The biological and physical stability and resilience of a selection of scottish soils to stresses, European Journal of Soil Science, 58(3), 811–821.

Laloy, E., and J. A. Vrugt (2012), High-dimensional posterior exploration of hydrologic models using multiple-try DREAM(ZS) and high-performance computing, Water Resources Research, 48(1), W01,526, doi:10.1029/2011WR010608.

Leitinger, G., E. Tasser, C. Newesely, N. Obojes, and U. Tappeiner (2010), Seasonal dynamics of surface runoff in mountain grassland ecosystems differing in land use, Journal of Hydrology, 385(1-4), 95–104.

Meurer, K., J. Barron, C. Chenu, E. Coucheney, M. Fielding, P. Hallett, A. M. Herrmann, T. Keller, J. Koestel, M. Larsbo, E. Lewan, D. Or, D. Parsons, N. Parvin, A. Taylor, H. Vereecken, and N. Jarvis (2020), A framework for modelling soil structure dynamics induced by biological activity, Global Change Biology, 26(10), 5382–5403, doi:https://doi.org/10.1111/gcb.15289.

Müller, K., Katuwal, S., Young, I., McLeod, M., Moldrup, P., de Jonge, L. W., & Clothier, B. (2018). Characterising and linking X-ray CT derived macroporosity parameters to infiltration in soils with contrasting structures. Geoderma, 313, 82-91.

Nawaz, M. F., G. Bourrié, and F. Trolard (2013), Soil compaction impact and modelling. A review, Agronomy for Sustainable Development, 33(2), 291–309, doi:10.1007/s13593-011-0071-8.

Oades, J. M. (1993), The role of biology in the formation, stabilization and degradation of soil structure, Geoderma, 56, 377–400, doi:10.1016/B978-0-444-81490-6.50033-9.

Oertel, C., J. Matschullat, K. Zurba, F. Zimmermann, and S. Erasmi (2016), Greenhouse gas emissions from soils - A review, Chemie der Erde - Geochemistry, 76(3), 327–352, doi:10.1016/j.chemer.2016.04.002.

Oldeman, L. R. (1992), Global extent of soil degradation, in Bi-Annual Report 1991-1992/ISRIC, pp. 19–36, ISRIC.

Or, D., and T. A. Ghezzehei (2002), Modelling post-tillage soil structural dynamics: a review, Soil and Tillage Research, 64(1-2), 41–59, doi:10.1016/S0167-1987(01)00256-2.

Or, D., F. J. Leij, V. Snyder, and T. a. Ghezzehei (2000), Stochastic model for posttillage soil pore space evolution, Water Resources Research, 36(7), 1641, doi:10.1029/2000WR900092.

Or, D., T. Keller, and W. H. Schlesinger (2021), Natural and managed soil structure: On the fragile scaffolding for soil functioning, Soil and Tillage Research, 208, 104,912, doi:https://doi.org/10.1016/j.still.2020.104912.

Rabot, E., M. Wiesmeier, S. Schlüter, and H. Vogel (2018), Soil structure as an indicator of soil functions : A review, Geoderma, 314, 122–137, doi:10.1016/j.geoderma.2017.11.009.

Richard, G., Cousin, I., Sillon, J. F., Bruand, A., & Guérif, J. (2001). Effect of compaction on the porosity of a silty soil: influence on unsaturated hydraulic properties. European Journal of Soil Science, 52(1), 49-58.

Romero-Ruiz, A. (2021), Geophysical Methods for Field-Scale Characterization of Soil Structure, Theses, Université de Lausanne.

Romero-Ruiz, A., N. Linde, T. Keller, and D. Or (2018), A review of geophysical methods for soil structure characterization, Reviews of Geophysics, 56(4), 672–697, doi:10.1029/2018RG000611.

Romero-Ruiz, A., N. Linde, L. Baron, S. G. Solazzi, T. Keller, and D. Or (2021), Seismic Signatures Reveal Persistence of Soil Compaction, Vadose Zone Journal, p. e20140, doi:https://doi.org/10.1002/vzj2.20140.

Romero-Ruiz, A., N. Linde, L. Baron, D. Breitenstein, T. Keller, and D. Or (2022), Lasting effects of soil compaction on soil water regime confirmed by geoelectrical monitoring, Water Resources Research, n/a(n/a), e2021WR030,696, doi:https://doi.org/10.1029/2021WR030696, e2021WR030696 2021WR030696.

Schjønning, P., Lamandé, M., Berisso, F. E., Simojoki, A., Alakukku, L., & Andreasen, R. R. (2013). Gas diffusion, non-Darcy air permeability, and computed tomography images of a clay subsoil affected by compaction. Soil Science Society of America Journal, 77(6), 1977-1990. https://doi.org/10.2136/sssaj2013.06.0224

Schjønning, P., J. J. H. van den Akker, T. Keller, M. H. Greve, M. Lamandé, A. Simojoki, M. Stettler, J. Arvidsson, and H. Breuning-Madsen (2015), Driver-Pressure-State-Impact-Response (DPSIR) analysis and risk assessment for soil compaction-A European perspective, in Advances in Agronomy, vol. 133, edited by D. Sparks and S. Hallock, chap. Chapter 5, pp. 183–237, Elsevier, doi:10.1016/bs.agron.2015.06.001.

Scholefield, D., and D. Hall (1986), A recording penetrometer to measure the strength of soil in relation to the stresses exerted by a walking cow, Journal of Soil Science, 37(1), 165–176.

Steinfeld, H., P. Gerber, T. D. Wassenaar, V. Castel, M. Rosales, M. Rosales, and C. de Haan (2006), Livestock's long shadow: environmental issues and options, Food & Agriculture Org.

Stewart, R. D., D. E. Rupp, M. R. Abou Najm, and J. S. Selker (2016), A Unified Model for Soil Shrinkage, Subsidence,and Cracking, Vadose Zone Journal, 15(3), doi:10.2136/vzj2015.11.0146.

Vereecken, H., A. Schnepf, J. Hopmans, M. Javaux, D. Or, T. Roose, J. Vanderborght, M. Young, W. Amelung, M. Aitkenhead, S. Allison, S. Assouline, P. Baveye, M. Berli, N. Brüggemann, P. Finke, M. Flury, T. Gaiser, G. Govers, T. Ghezzehei, P. Hallett, and K. Lamorski (2016), Modelling soil processes: review, key challenges and new perspectives, Vadose Zone Journal, 15(5), doi:10.2136/vzj2015.09.0131.

Vyalov, S. S. (2013). Rheological fundamentals of soil mechanics. Elsevier.

Whalley, W., G. Matthews, and S. Ferraris (2012), The effect of compaction and shear deformation of saturated soil on hydraulic conductivity, Soil and Tillage Research, 125, 23–29.

Wu, L., McGechan, M. B., McRoberts, N., Baddeley, J. A., & Watson, C. A. (2007). SPACSYS: integration of a 3D root architecture component to carbon, nitrogen and water cycling—model description. Ecological Modelling, 200(3-4), 343-359.

Yi, J., Hu, W., Beare, M., Liu, J., Cichota, R., Teixeira, E., & Guo, L. (2022). Treading compaction during winter grazing can increase subsequent nitrate leaching by enhancing drainage. Soil and Tillage Research, 221, 105424.

Figures

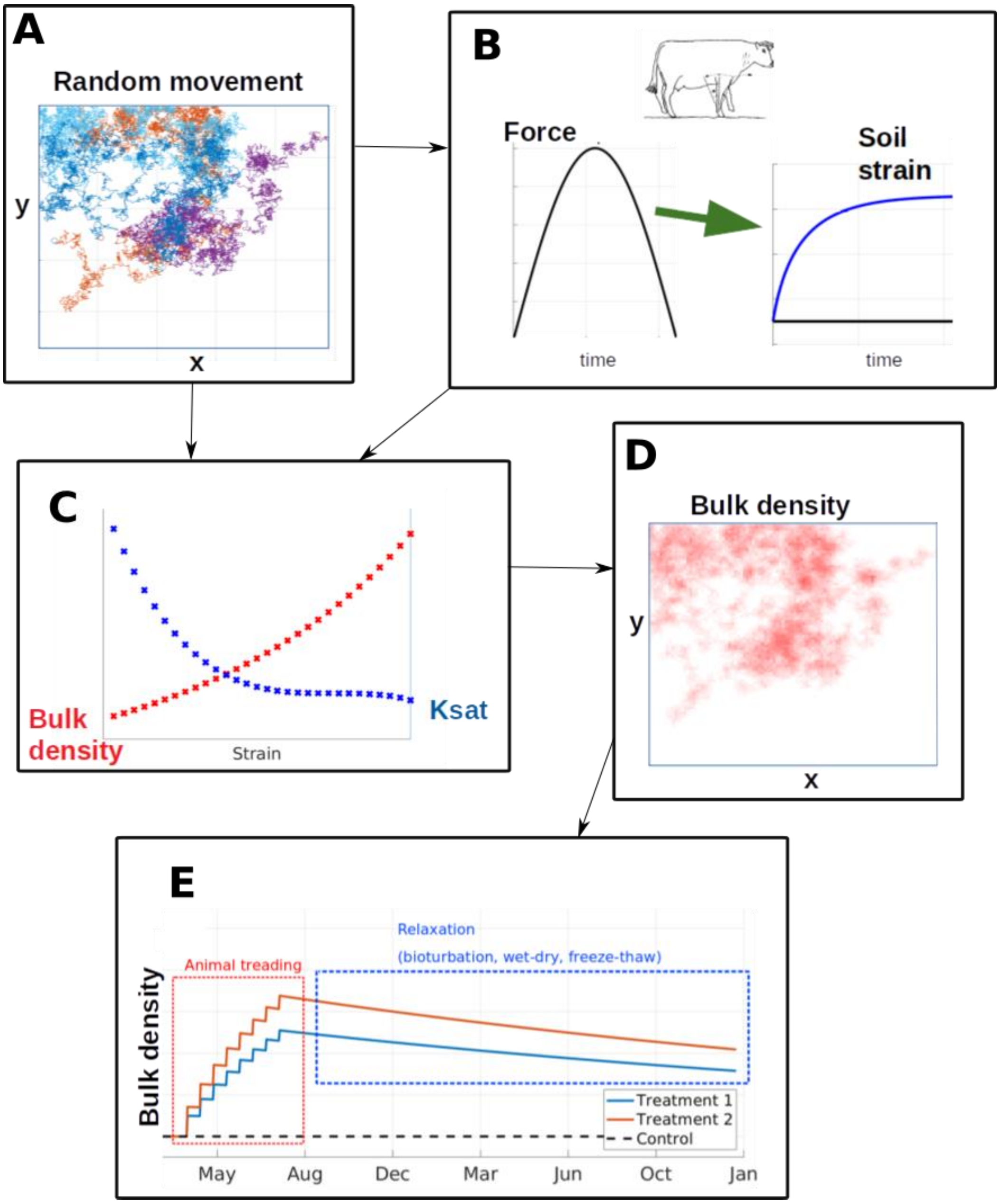

Figure 1

Diagram illustrating the main elements of the soil compaction model presented in this work. In A, animal movement in a limited area is simulated obtaining number of steps for a given soil cell. In B, a soil rheology model is used to calculate the soil strain as a function of the steps calculated. In C, soil physics models are used to obtain soil physical properties as a function of the strain. In D, we illustrate that this is done spatially so there is a change in bulk density for all cells in the models. In E, we illustrate how bulk density changes as a function of time for a given cell.

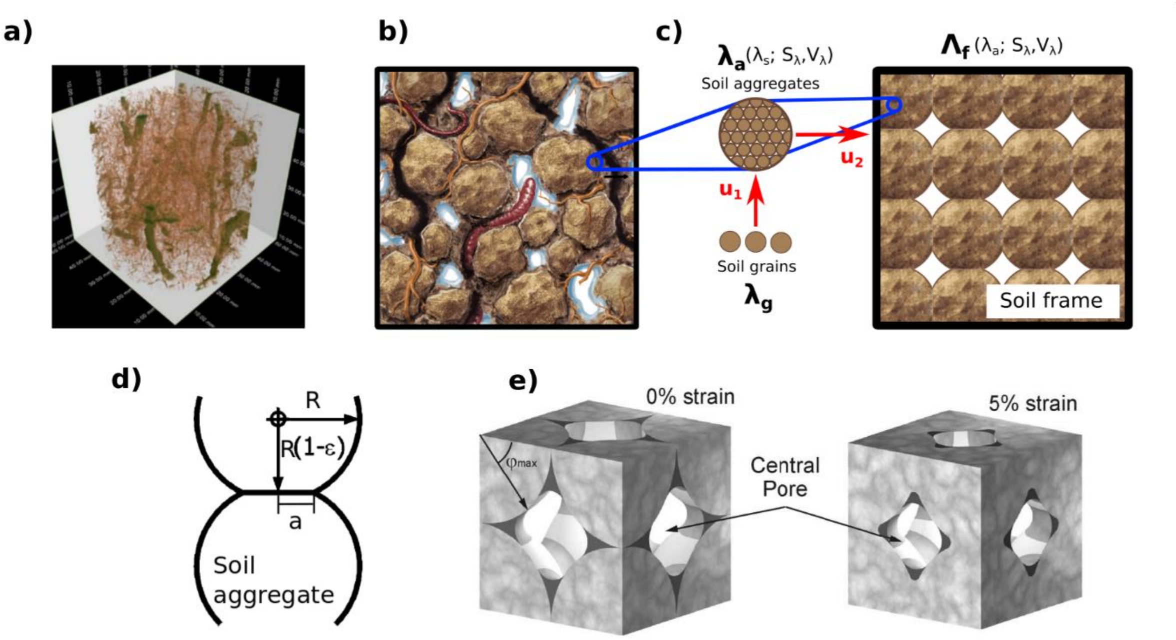

Figure 2

Conceptual model of soil structure. (a) Computer tomography of a 100 cm^3 soil sample from an agricultural soil (voxel size 60 μm, corresponding to a minimum pore width of 120 μm) (from Keller et al., 2017). (b) Conceptual illustration of a structured soil including aggregation and macroporosity created by biological activity (from Romero-Ruiz et al., 2018). (c) Schematic representation of the upscaling of soil physical properties of structured soils from soil grains to soil aggregates and ultimately to a soil frame (from Romero-Ruiz, 2021). In these representations the soil is dry. (d) Schematic representation of deformation of contacts between aggregates due to compaction. (e) Illustration of volume reduction and pore closure due to compaction-induced viscous strains.

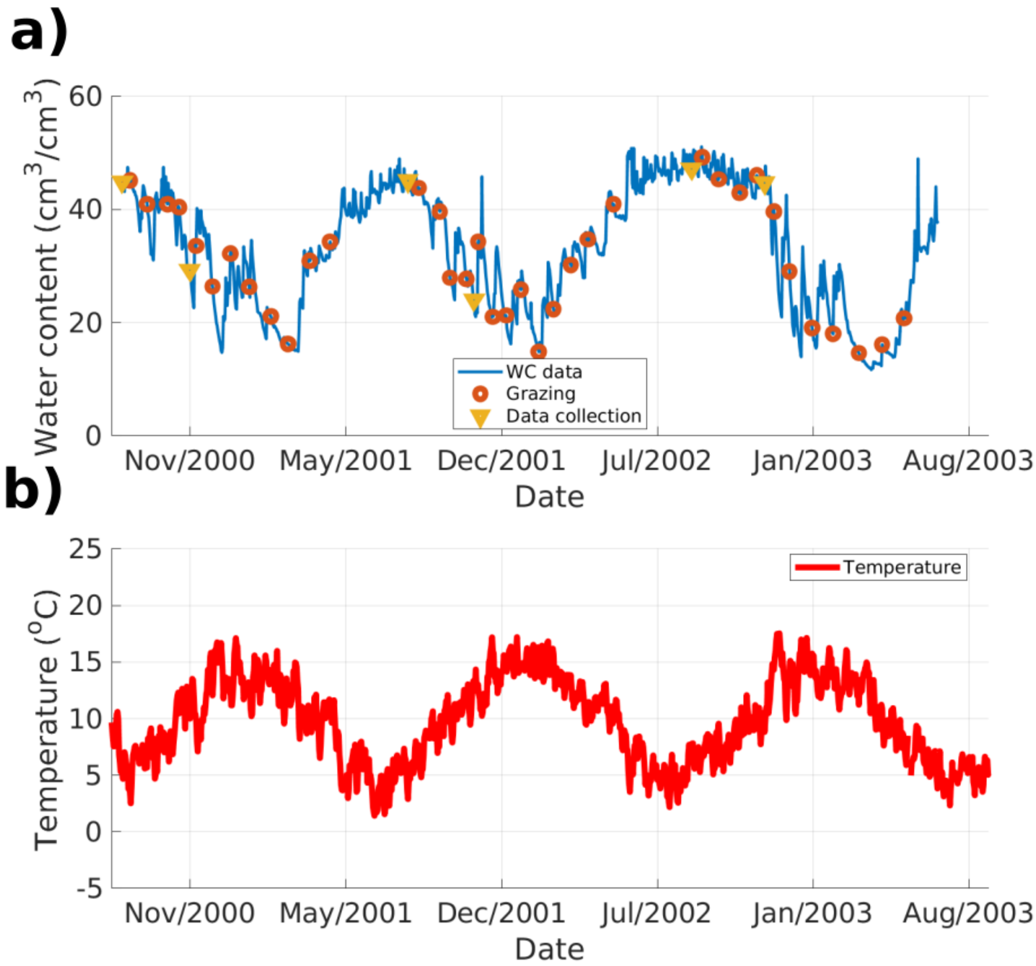

Figure 3

(a) Volumetric water content and (b) soil temperature at 10 cm depth measured at the Tussock Creek study site. In (a), the grazing dates are marked with circles and the pre- and post-spring data collection dates are marked with triangles.

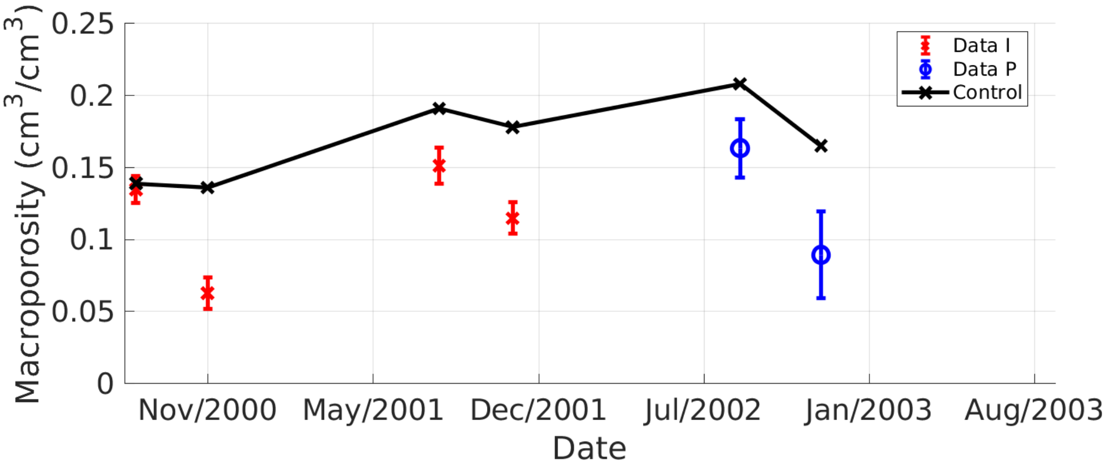

Figure 4

Temporal changes in soil macroporosity values measured at the Tussock Creek study site. The data were averaged for various grazing treatments: normal grazing of undrained land (UND), conventional grazing (CON), conventional grazing, but restricted to 3 hours for grazing events during autumn (AUT), conventional grazing, but restricted to 3 hours grazing when the soil is wet (THR), and conventional grazing, but scheduled to never take place when the soil was wet (NPG).. Error bars correspond to standard deviations. Control (NIL grazed) data are presented for reference. Data were taken from Houlbrooke et al. (2009). Data I corresponds to the data used for parameter calibration and Data P are data predicted for model validation.

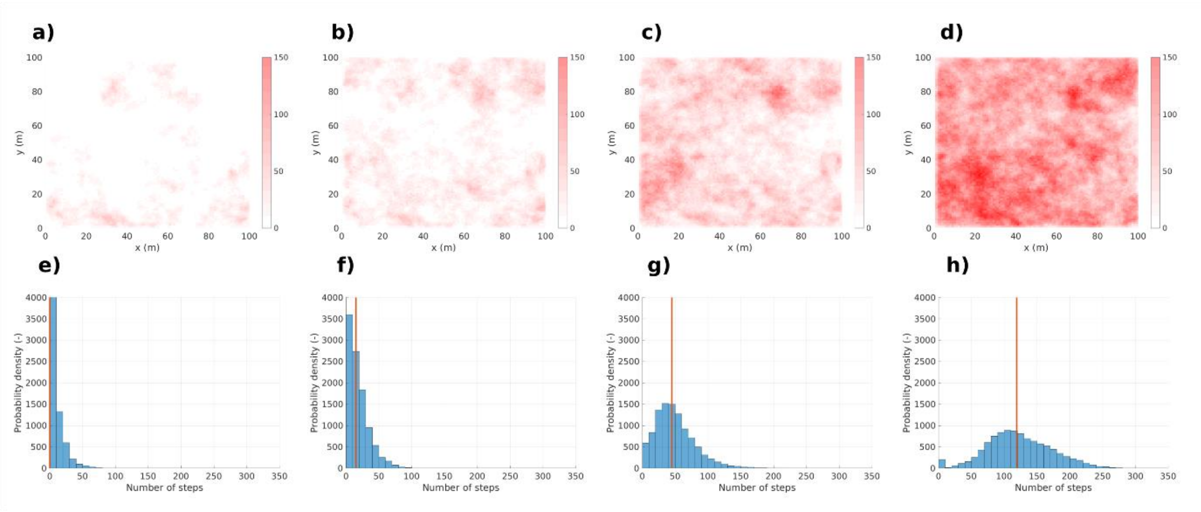

Figure 5

Maps of simulated number of steps for days (a) 1, (b) 3, (c) 8 and (d) 22 in a grazing period. For illustration purposes, we chose a stock density of four animals per hectare and considered 5000 steps per animal per day. (e) 1, (f) 3, (g) 8 and (h) 22 present the histograms of the number of steps associated with (a), (b), (c) and (d), respectively. The median value of the obtained distributions is highlighted for each case.

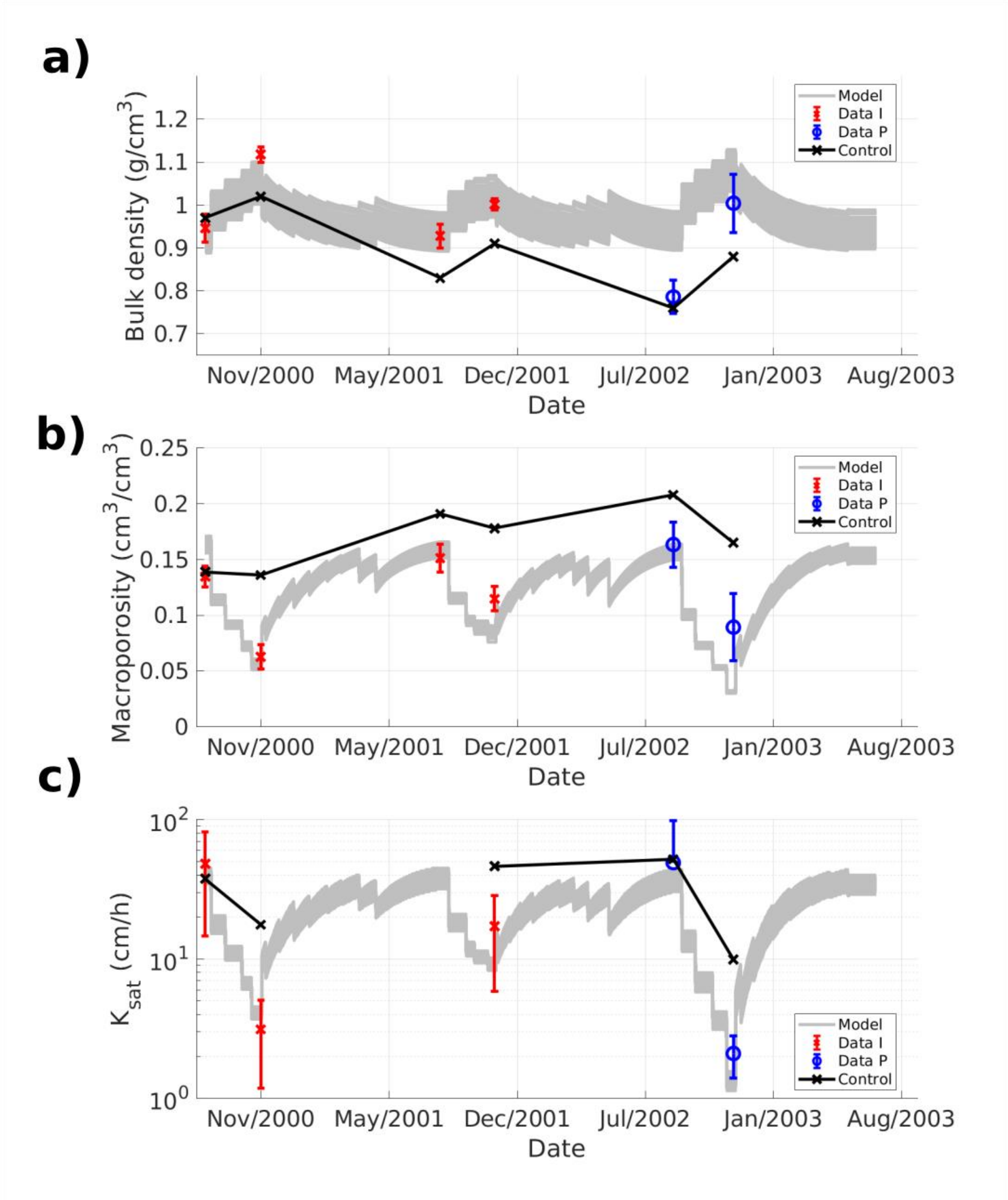

Figure 6

Modelled and measured (a) bulk density, (b) macroporosity and (c) saturated hydraulic conductivity values at 0-5 cm soil depth. Control data (non-grazed) are presented for reference. Data I corresponds to the data used for parameter calibration and Data P are data predicted for model validation. The curves in grey are all modelled solutions after burn-out resulting from the Markov-Chain Monte Carlo inversion.

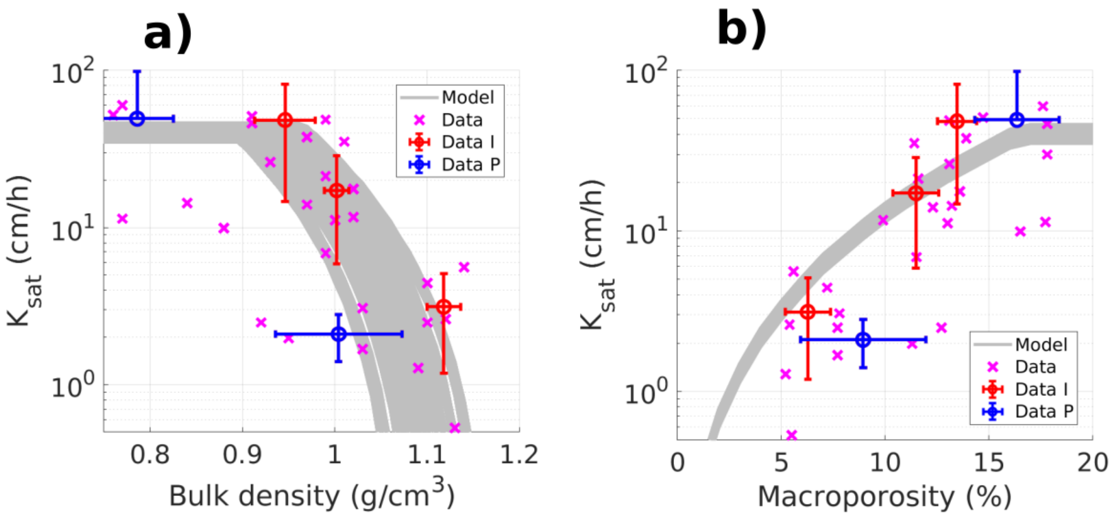

Figure 7

Modelled and measured saturated hydraulic conductivity as a function of (a) bulk density and (b) macroporosity. The figure contains all data presented by Houlbrooke et al., (2009), data used in this analysis for parameter calibration (Data I) and data predicted for model validation (Data P). The curves in grey are all modelled solutions after burn-out resulting from the Markov-Chain Monte Carlo inversion.